Case Studies in Construction Materials 14 (2021) e00526

Contents lists available at ScienceDirect

Case Studies in Construction Materials

journal homepage: www.elsevier.com/locate/cscm

Case study

Effect of scale-up on the properties of PCM-impregnated tiles containing glass scraps

Chiara Molinari[a,*], Chiara Zanelli[a], Luca Laghi[b], Giulia De Aloysio[b], Mattia Santandrea[b], Guia Guarini[a], Sonia Conte[a], Michele Dondi[a]

[a] ISTEC-CNR, Istituto di Scienza e Tecnologia dei Materiali Ceramici, Via Granarolo 64, 48018, Faenza, Italy
[b] CertiMaC scarl, Via Ravegnana 186, 48018, Faenza, Italy

ARTICLE INFO

Article history:
Received 12 November 2020
Received in revised form 5 February 2021
Accepted 3 March 2021

Keywords:
Bloating
Glass scraps
Lightweight aggregates
Phase change material
Scale-up

ABSTRACT

In the latest years, the interest about Phase Change Materials (PCM) in building applications grew in force of their capability to adsorb heat and limit in-out building heat exchanges. The main problem is how to introduce PCM into the building envelope, also in case of ventilated façades. For this purpose, a ceramic foam was studied. Two different batches based on porcelain stoneware and soda-lime glass scraps were prepared to understand the involved bloating phenomena. Suitable bulk density and porous microstructure were achieved by adding a foaming agent and batch optimization. Specimen size was scaled up (from ∅ 3 cm to 15 × 15 cm) and its effect on bloating, PCM incorporation, and thermal properties was studied. Furthermore, different firing temperatures and heating rates were evaluated. The whole study was focused to disclose possible drawbacks in the industrial transfer of the PCM-bearing composite production.

1. Introduction

The most energy consuming sector in the European Union, responsible of about the 36 % of the produced carbon dioxide, is the building sector [1]. The continuous increase of the urbanization combined with the global warming phenomenon, that is leading to a fast growth of indoor cooling, requires a transition from traditional structures to Nearly Zero-Energy edifices [2,3]. Among the different technological solutions to improve the thermal comfort, Phase Change Materials (PCM) can play an important role [4]. With this purpose, the scientific literature has focus the attention on PCM – enhanced building applications, from both modelling and experimental perspectives [5–7]. In force of the high energy storage density of these latent heat-based systems, it is possible to reduce the gap between energy demand and supply [8,9]. The effect related to the incorporation of PCM within the building envelope was already studied [10–12].

Respect to other materials, organic compounds (like paraffins and fatty acids) have several advantages, like no solidification subcooling, low hysteresis and higher stability [13,14]. To ensure the full solidification and regeneration during the hot season, the implementation into ventilated façades can be realized [15–17].

The inclusion of PCM can be achieved by different techniques, like direct incorporation [18], immersion [19] encapsulation [11,20,21] and shape stabilization [22]. Cement, mortars, and perforated bricks are the most studied materials

* Corresponding author.
E-mail addresses: chiara.molinari@istec.cnr.it (C. Molinari), chiara.zanelli@istec.cnr.it (C. Zanelli), l.laghi@certimac.it (L. Laghi), g.dealoysio@certimac.it (G. De Aloysio), m.santandrea@certimac.it (M. Santandrea), guia.guarini@istec.cnr.it (G. Guarini), sonia.conte@istec.cnr.it (S. Conte), michele.dondi@istec.cnr.it (M. Dondi).

https://doi.org/10.1016/j.cscm.2021.e00526

[12–26], while studies considering the use of PCM in porous tiles are rather scarce [27]. Among the possibilities mentioned, only the immersion technique can be used to incorporate PCM into a ceramic porous structure, improved by operating under vacuum [28–30]. The pore formation in a ceramic matrix can be achieved by adding several additives [31,32]. A foaming agent can be used to obtain a large porosity useful for PCM storage. To improve bloating, the addition of glass scraps can be tuned [33]. The production of glass-based foams must face several problems correlated to the difficult predictability of bloating and shape stability that complicate scale-up procedures [34]. Despite the increasing literature, nowadays there are not conclusive experimental studies that concern PCM on real scale building applications. Numerical modelling and pilot devices remain today the most used tools for assessing the behaviour of the PCM in construction [35–38]. The goal of this work is to obtain PCM-containing lightweight ceramic tiles for ventilated façades in view of industrial production. The main focus of the work was primarily pointing out the effects of process parameters and scale up on the bloating phenomenon and on the fired properties involved in the definition of thermal characteristics.

2. Materials and methods

The choice of materials was aimed at facilitating the technological transfer to industry and the reuse of wastes. Starting from a commercial porcelain stoneware spray-dried powder, mixtures were obtained by dry mixing with other components. Soda-lime glass scraps were added in order to achieve bloating in a temperature range compatible with the industrial practice. Cullet glasses were previously crushed and sieved till particle size lower than 100 μm. The chemical composition of raw materials is reported in Table 1.

Bulk density and thermal conductivity for porcelain stoneware specimen fired at 1150 °C are reported in Table 2. The uncertainty associated to the thermal conductivity value was estimated by using the model developed in [39].

Polishing sludges, generally containing some SiC from abrasive tools that acts as expanding agent, were reproduced by SiC addition. To boost bloating, a second mixture was prepared by addition of dolomite. Both formulations are reported in Table 3.

A water solution of polyethylene glycol (PEG, 3% w/w) was added to favour particles adhesion during shaping to all the formulations (6 wt%). Samples were formed by uniaxial pressure (15 MPa): circular specimens were pressed with a laboratory hydraulic press (Nannetti) by using molds of 30 or 60 mm in diameter; rectangular and square tiles were obtained by a customized press (Giuliani) using 115 × 120 mm and 150 × 150 mm molds. Once dried at 120 °C for 8 h, specimens were fired at 950, 1000, 1075 and 1150 °C. Two different thermal cycles with electric kiln were set up. To simulate the industrial conditions, fast firing was carried out by heating at 40 °C/min till maximum temperature, maintained for 5 min. To point out the effect of process parameters, also a slow firing process was performed, with a heating rate of 2.5 °C/min till maximum temperature without any dwell time. The phase composition was determined by X-ray powder diffraction (Bruker, D8 Advance with LynxEye detector, 0.02°2θ sampling interval over the 10–100°2θ range). The experimental error is within 2 % relative. Fired specimens were characterized by water absorption, total porosity, bulk density (ISO 10545-3) and linear bloating, as $100\cdot(L_f\text{-}L_m)/L_m$, where L_f is the diameter/length of the fired sample and L_m is the mold diameter/length. Microstructure was studied using a digital microscope HIROX RH-2000. To prevent obstacles to impregnation due to air presence within porosity, rectified foams were immersed into melted PCM, under vacuum, for 30 min. After impregnation, the excess of PCM on the surface specimen was manually removed and the specimens were cooled and conserved at about 4 °C. An impregnation efficiency parameter was defined as: volume of PCM impregnated / volume of the specimen * 100.

The thermal performance was determined by means of a guarded heat flow meter (DTC 300, TA Instrument) on rectified specimens with diameter of 50.8 ± 0.3 mm and thickness of 7.5 mm. This test method is based on a steady-state technique for assessing the resistance to thermal transmission (thermal resistance) of samples with thickness lower than 25 mm. The thermal resistance and the thermal conductivity of the samples were evaluated taking into account an average test temperature of 10 °C and after calibrating the guarded heat flow meter on reference samples with certified properties. Available calibration samples are characterized by thermal resistance values ranging from 0.0005 to 0.05 m^2 K/W. During the experimentation, the sample to be tested is held under a reproducible compressive load between two polished metal surfaces, each controlled at a different temperature so that heat can flow through the test stack. The compressive axial load, which is provided through a pneumatic cylinder, is necessary to minimize the interface thermal resistance and to produce during testing the same sample contact resistance as during calibration. The lower contact surface is part of a calibrated heat flux transducer. An axial temperature gradient is established in the stack as heat flows from the upper surface through the sample to the lower surface. A guard surrounding the test stack is kept at the uniform mean temperature of the two plates, so as to minimize lateral heat flow to and from the stack. After reaching thermal equilibrium, the temperature difference across the specimen is measured together with the output from the heat flow transducer. These values and the specimen thickness are then used to calculate the thermal conductivity. The thermal conductivity of the PCM was measured by means of the aforementioned heat flow meter (DTC 300, TA Instrument), while the melting and the solidification temperatures together with the latent heat capacity of melting and freezing of the PCM were experimentally determined by employing a Differential Scanning Calorimeter (DSC 250, TA Instrument). The DSC analysis were carried outby employing a heating ramp between 0 °C and 60 °C and a cooling ramp - between 60 °C and 0 °C- so as to assess the melting and solidification points, with relevant temperatures and latent heats, respectively. The heating and cooling rates were equal to 10 °C/min. The DSC 250 apparatus is based on Modulated DSC (MDSC), a technique for measuring the difference in heat flow between a sample and an inert reference as a function of time and temperature. In MDSC a different heating profile (temperature regime) is applied to the

Table 1
Chemical composition of tested materials.

Wt%	Porcelain stoneware	Soda-lime glass
SiO_2	73.41 ± 0.20	71.70 ± 0.20
TiO_2	0.67 ± 0.05	0.07 ± 0.01
Al_2O_3	17.08 ± 0.20	2.70 ± 0.05
Fe_2O_3	1.47 ± 0.05	0.42 ± 0.05
MgO	0.51 ± 0.05	2.00 ± 0.05
CaO	0.99 ± 0.05	9.49 ± 0.01
Na_2O	3.37 ± 0.10	12.40 ± 0.20
K_2O	1.94 ± 0.10	1.01 ± 0.05

Table 2
Physical properties for stoneware specimen fired at 1150 °C.

Bulk density [g/cm^3]	Thermal conductivity [W/mK]
1.91 ± 0.01	0.78 ± 0.04

Table 3
Formulation of experimental bodies.

Raw materials [wt%]	Sample A	Sample B
Porcelain stoneware	49	39
SiC	1	1
Soda-lime glass	50	50
Dolomite	–	10

sample and reference. In particular, a sinusoidal modulation (oscillation) is overlaid on the conventional linear heating or cooling ramp in order to determine a profile where the average sample temperature continuously changes with time, but not in a linear manner. By imposing this more complex heating profile on the sample, the same effect is obtained as if two experiments were conducted simultaneously on the material - one experiment at the traditional linear (average) heating rate and one at a sinusoidal (instantaneous) heating rate. On the basis of the above-described procedure, the MDSC method has several significant advantages compared to conventional DSC, such as:

- Separation of complex transitions into more easily interpreted components
- Improved resolution without compromising sensitivity
- Improved sensitivity to detect weak transitions
- Determination of heat flow and heat capacity in a single experiment

The elaborations were performed through the TRIOS Software (TA Instruments).

3. Results and discussion

3.1. Foam optimization

The sole addition of SiC to porcelain stoneware did not induce bloating between 950 and 1150 °C. To obtain SiC oxidation, glass scraps were added to the formulation, leading to achieve an adequate amount of a low viscosity melt in the desired temperature range [34]. In fact, the addition of glass favors the reactivity of SiC particles [40]. Both batches were fired from 950 to 1150 °C, mimicking the industrial process with the fast firing rate. As observed by XRD analysis, for both systems the higher the firing temperature, the larger was the amount of the vitreous phase (Table 4). This trend is slightly more pronounced in the B mixture. Both formulations show bloating throughout the range studied but with different extents. The effect of batch formulation on the obtained microstructure as a function of firing temperature is reported in Fig. 1.

A first common aspect is the role played by the ceramic powder. It is easy to see that at lower temperatures particles spray-dried powders act as a sort of skeleton, and reactions with the glassy phase seem to be limited. At 950 °C, both formulations show a scarce bloating, characterized by the presence of small pores, up to 1 mm in diameter. The addition of dolomite caused a simultaneous increase in pore size (up to 5) and number of smaller pores (<10 μm).

The dissolution of SiC is constrained by high viscosity of the melt that reduced the bloating efficiency [34]. The temperature growth promoted bloating, especially in the B batch. This effect is conspicuous for all specimens fired at 1150 °C. Such a high temperature fostered a dissolution of spray-dried agglomerates and reduced the melt viscosity, promoting SiC

Table 4
Phase composition (wt%) of A and B bodies as a function of firing temperature.

Firing temperature	950 °C		1000 °C		1150 °C	
Batch	A	B	A	B	A	B
Quartz	12.5 ± 0.2	11.5 ± 0.1	12.4 ± 0.3	9.9 ± 0.1	10.6 ± 0.2	8.8 ± 0.1
Wollastonite	4.2 ± 0.1	4.6 ± 0.1	4.3 ± 0.1	5.2 ± 0.1	–	3.5 ± 0.1
Plagioclase	8.5 ± 0.2	10.9 ± 0.2	8.6 ± 0.2	10.3 ± 0.2	7.8 ± 0.1	6.0 ± 0.1
K-feldspar	3.4 ± 0.1	2.1 ± 0.1	0.5 ± 0.1	2.2 ± 0.1	–	–
Illite	0.6 ± .01	2.1 ± 0.1	–	–	–	–
Vitreous phase	70.8 ± 0.7	68.8 ± 0.6	74.2 ± 0.7	72.5 ± 0.5	81.6 ± 0.3	81.7 ± 0.3

reactivity and eventually bloating. The body A exhibits a texture with pores up to 15 mm, while for the B mix the pore size is importantly increased by dolomite breakdown, forming pores up to 20 mm.

The dolomite decomposition enhanced the specimen bloating [41]. A secondary porosity is observed, formed by small pores (<1.5 mm) within the septa between bigger bubbles. As a result of the larger expansion, septa in the B specimen appear

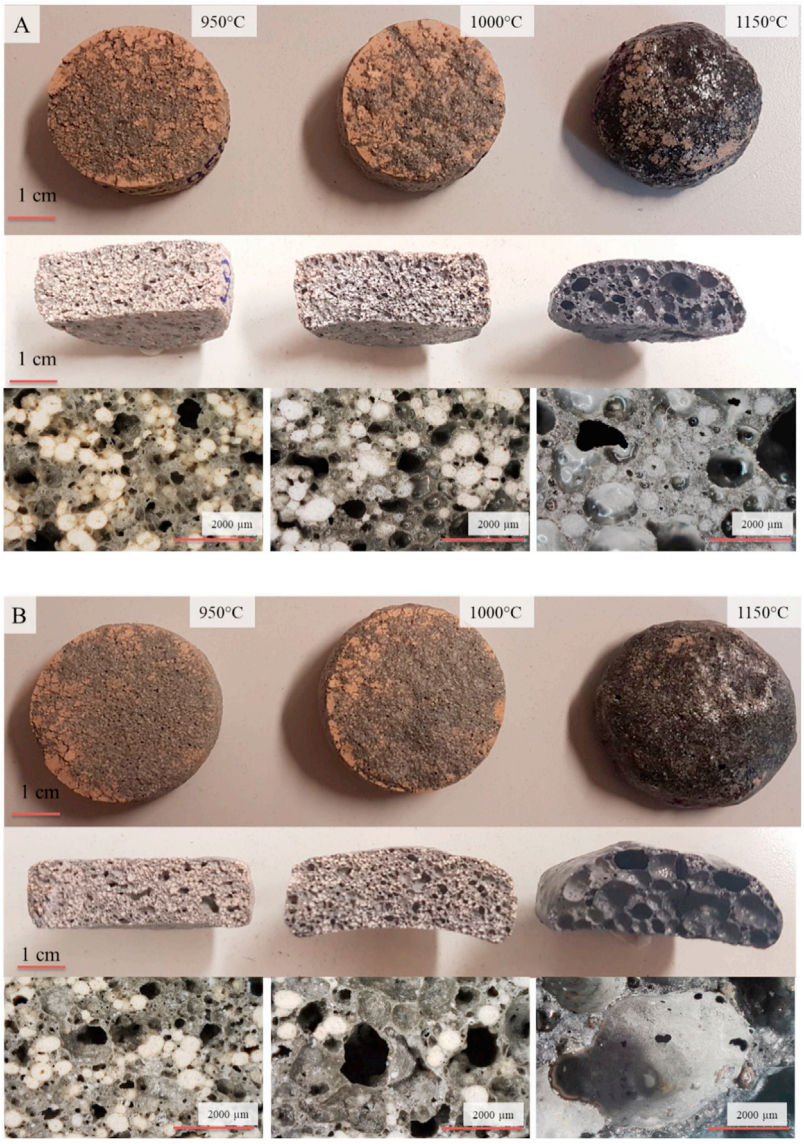

Fig. 1. Effect of firing temperature on macro and microstructure for A and B formulations; mold Ø 3 cm – rapid firing cycle. Microstructures color guide; white: ceramic agglomerates; gray: glassy matrix; black: pores.

to be thinner, generating an interconnected secondary porosity. The combination of skeleton dissolution and melt viscosity reduction led to a progressive structural collapse.

The effect of firing on the specimen properties can be followed by taking bulk density as a proxy, fundamental to optimize materials bloating (Fig. 2). The minimum bulk density registered by the A formulation was increased after the addition of dolomite. Its decomposition leads to a second independent bloating mechanism, shifting the optimal temperature from 1000 to 1075 °C. The SiC oxidation increased the internal gas pressure, boosting the specimen expansion and favoring the formation of an open porosity. At the same time, pores size and shape depend on viscosity and surface tension of the melt, which control bubbles growth and coalescence [44].

The microstructure of the two batches at the minimum bulk density is clearly different, due to distinct bloating mechanisms, gas amounts available and glassy phase properties. As the bloating observed is ruled by kinetics, heating rate plays an important role in the determination of final microstructure. A drastic increase of firing time favors as the carbide/carbonate decomposition, as the pore expansion, ultimately favoring bloating. When fired at 1075 °C with a heating rate of 2.5 °C/min, each formulation underwent to a similar bloating, which gave rise to a bulk density reduction slightly more important for the A mix than the B one (Table 5).

As reported for the B samples, the gas leakage through the interconnected porous structure is favored by the higher firing time at 100 °C (Fig. 3). Indeed, the presence of a sintered glass layer at 1075 °C retained the formed gas, achieving a more efficient bloating [41]. By the way, no further improvement occurred by increasing the temperature, due to the progressive specimen collapse.

3.2. PCM properties

The DSC analysis for PCMs was carried out on three samples, tested at the same conditions. Fig. 4 shows the DSC thermogram of one of these specimens. It can be clearly observed a peak (minimum) corresponding to the melting temperature of the PCM and a peak (maximum) corresponding to the solidification temperature of the PCM. The melting and solidification temperatures, obtained as the average value of the measures performed on three specimens, resulted equal to 29.9 °C and 19.3 °C, respectively, while the heat capacity of melting and freezing, obtained as the average value of the three specimens, resulted equal to 205 kJ/kg and 203 kJ/kg. The measures performed in DTC allowed to determine the thermal conductivity of PCM that resulted equal to 0.216 W/mK in liquid phase and 0.280 W/mK in solid phase.

3.3. PCM impregnation and thermal properties

Several aspects must be considered to define the conditions necessary to obtain an optimized composite product. The final thermal properties are not only related to number and size of pores, but most importantly to the quantity of PCM that can be incorporated in the ceramic foam, defined as impregnation efficiency. In order to point out the effect of firing cycle parameters on impregnation efficiency, A and B samples were fired at 1075 °C and 1150 °C using both rapid and slow firing cycles. Fired specimens were surface ground, impregnated under vacuum, and the amount of incorporated PCM was expressed as percent of the foam impregnated. The results obtained show different trends (Table 6).

Every batch has an impregnated volume that turns lower by increasing the firing temperature. As already discussed, the progressive reduction of melt viscosity induced a porosity decrease, so limiting the maximum volume available. At the same time, the presence of bigger pores makes more difficult the retention of melted PCM after the impregnation process. Regardless the increased bloating observed in each batch, the reduction of heating rate produced a different effect in the mixes under study. In the A specimens, it brought about a lower impregnation efficiency. On the contrary, B mixes are characterized by an increased impregnation efficiency, higher than the corresponding value in the A sample. From this standpoint, it is possible to conclude that the optimal firing conditions are strongly dependent on the batch composition [42]. This leads to a specific porous structure accessible to melted PCM.

The addition of PCM to the ceramic foams modifies the thermal conductivity of the material. Fig. 5 shows the thermal conductivity of specimens before and after impregnation. It can be observed, through a linear regression of data, that specimens impregnated with PCM have lower values of thermal conductivity in the 600−1400 kg/m^3 range. However, additional data are needed to confirm this trend.

3.4. Scale up of the PCM-containing foam

According to the preliminary results, optimal firing conditions for the scale-up of foams were defined in terms of bulk density, impregnation efficiency and thermal conductivity. Given to the lower bulk density and the quite constant thermal conductivity of the impregnated foams, the B formulation was selected. Firing was chosen at 1075 °C with a slow heating rate. Ceramic foams, as obtained after the rectification process, are reproduced in Fig. 6.

Account must be taken that the mold size affects bloating and particularly the increase of specimen size limits the volume useful for impregnation, even though the total porosity is increased (Table 7). At the same time, the total porosity tends to a constant value by increasing the specimen volume. A similar trend is observed about the impregnation efficiency, which is affected by sample dimensions only to a little extent (Table 5). The increase of specimen size gave rise to a decrease of volume impregnation of about 15 %, because of a volume increase of 1500 %.

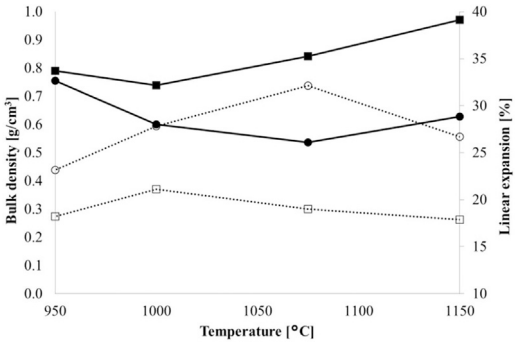

Fig. 2. Effect of firing temperature on the properties of 3 cm specimens. Experimental uncertainty is within the symbol size. ■ A bulk density; ● B bulk density; □ A linear expansion; ○ B linear expansion.

Table 5
Effect of heating rate on the physical properties for A and B batches fired at 1075 °C: difference measured (as percent change) passing from 40 to 2.5 °C/min.

Changes of physical properties (%)	Sample A	Sample B
ΔLinear expansion	+48	+36
ΔWater absorption	+32	+30
ΔBulk density	−51	−43
ΔTotal porosity	+12	+11

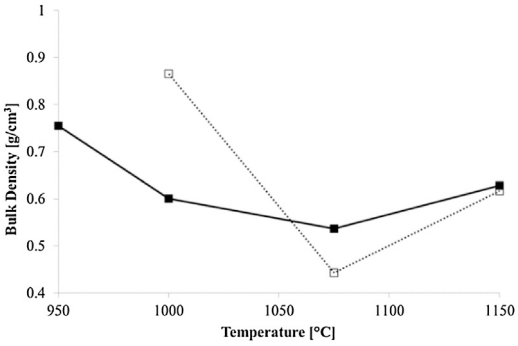

Fig. 3. Effect of firing rate on bulk density (batch B): ■ Rapid firing cycle; □ Slow firing cycle.

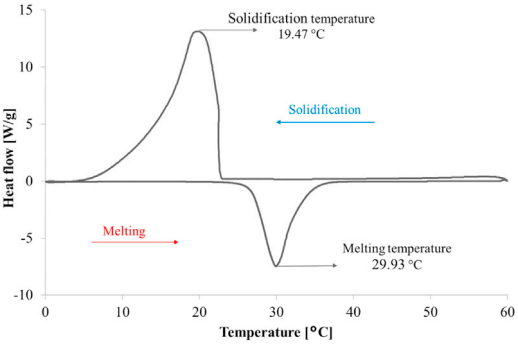

Fig. 4. DSC analysis on a PCM sample.

Table 6
Effect of firing parameters on impregnation efficiency for A and B formulation.

Heating rate [°C/min]	Impregnation efficiency			
	A		B	
2.5	36.5	–	36.4	–
40	46.2	30.8	22.9	16.8

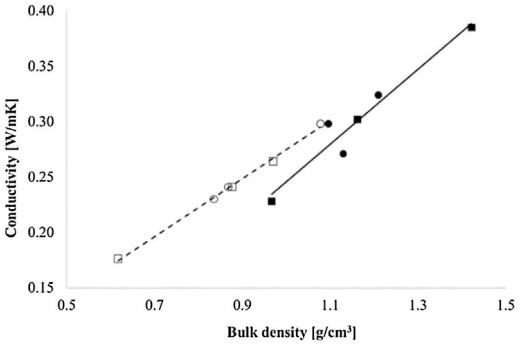

Fig. 5. Thermal conductivity of specimens before and after impregnation with PCM; ○ A formulation befor impregration; □ B formulation before impregnation; ● A formulation after impregration; ■ B formulation after impregration; — Linear regression befor impregration; ▬ Linear regression after impregration.

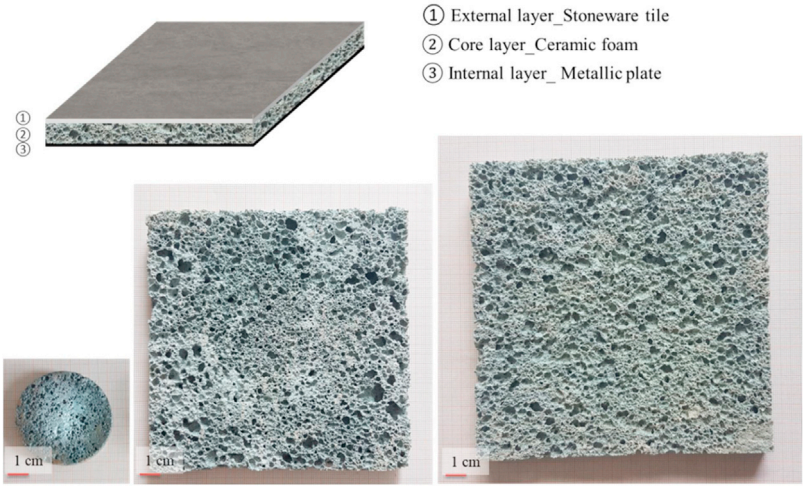

Fig. 6. Scaled ceramic foams after rectification.

Table 7
Effect of scale up on the properties of fired specimens.

Mold size [mm]	Bulk density [g/cm^3]	Total porosity [v/v%]	Volume of rectified sample [cm^3]	Volume impregnated [%]
∅30mm	0.35	86	Not available	Not available
∅60mm	0.51	69	15.1	39
115 × 120 mm	0.39	85	246.1	24
150 × 150 mm	0.46	82	377.5	26

4. Conclusions

The present study demonstrates the scale-up feasibility to produce PCM-containing porous ceramic tiles. The effect of firing process on the final product properties and potential drawbacks were pointed out. The most important parameter that must be tuned is the chemical composition of the batch, which determines the stability of SiC into the melt formed at high

temperature. At the same time, the batch composition is responsible of the physical properties of the melt, which in turn modulate the bloating performance. For this purpose, the use of waste materials is highly challenging. The introduction of dolomite let to increase the firing temperature and boosted the bloating phenomena. The best composition was used to define the optimal firing conditions to maximize both bulk density reduction and amount of PCM that can be incorporated in the tile. However, several drawbacks are intrinsically linked to the mechanism of formation of the porous structure. Future work must investigate in depth the thermal properties and heat absorption properties of the obtained composite materials. Given by the particular structure of the ceramic foam, an important part of the future work will be focused on the engineering of a complex device comprehensive of the PCM-containing foam.

Funding

This work was supported by Emilia-Romagna Region [Project INVOLUCRO - CUP J42F17000130009 - POR FESR 2014-2020 (Axis 1, Action 1.2.2)].

Declaration of Competing Interest

The authors declare that they have no known competing financial interests or personal relationships that could have appeared to influence the work reported in this paper.

References

[1] Directive (EU) 2018/844 of the European Parliament and of the Council of 30 May 2018 amending Directive 2010/31/EU on the energy performance of buildings and Directive 2012/27/EU on energy efficiency.
[2] International Energy Agency, The Future of Cooling: Opportunities for Energy-efficient Air Conditioning, (2018) Available from:.
[3] A. Kasaeian, H. Sarrafha, Chapter 3 - solar energy systems: an approach to zero energy buildings, in: A.K. Azad (Ed.), Advances in Clean Energy Technologies, Elsevier Inc., Amsterdam, 2021, pp. 89–170, doi:http://dx.doi.org/10.1016/B978-0-12-821221-9.00003-7.
[4] G. Gholamibozanjani, M. Farid, A comparison between passive and active PCM systems applied to buildings, Renew. Energy 162 (2020) 112–123.
[5] B. Duraković, PCM-based building envelope systems, Innovative Energy Solutions for Passive Design, Springer International Publishing, Switzerland, 2020, doi:http://dx.doi.org/10.1007/978-3-030-38335-0.
[6] F. Cabeza, A. de Gracia, 20 - thermal energy storage systems for cooling in residential buildings, in: L.F. Cabeza (Ed.), Advances in Thermal Energy Storage Systems (Second Edition) Methods and Applications, Woodhead Publishing Series in Energy, Elsevier Inc., Amsterdam, 2020, pp. 595–623, doi: http://dx.doi.org/10.1016/C2019-0-00061-1.
[7] L. Boussaba, G. Lefebvre, S. Makhlouf, A. Grados, L. Royon, Investigation and properties of a novel composite bio-PCM to reduce summer energy consumptions in buildings of hot and dry, Sol. Energy 214 (2021) 119–130.
[8] V.V. Rao, R. Parameshwaran, V.V. Ram, PCM-mortar based construction materials for energy efficient buildings: a review on research trends, Energy Build. 158 (2018) 95–122.
[9] M. Song, F. Niu, N. Mao, Y. Hu, S. Deng, Review on building energy performance improvement using phase change materials, Energy Build. 158 (2018) 776–793.
[10] L.F. Cabeza, A. Castell, C. Barreneche, A. de Gracia, A.I. Fernández, Materials used as PCM in thermal energy storage in buildings: a review, Renew. Sust. Energ. Rev. 15 (2011) 1675–1695.
[11] P.K.S. Rathore, S.K. Shukla, Potential of macroencapsulated pcm for thermal energy storage in buildings: a comprehensive review, Constr. Build. Mater. 225 (2019) 723–744.
[12] L. Navarro, A. de Gracia, D. Niall, A. Castell, M. Browne, S.J. McCormack, P. Griffiths, L.F. Cabeza, Thermal energy storage in building integrated thermal systems: a review. Part 2. Integration as passive system, Renew. Energy 85 (2016) 1334–1356.
[13] M.M. Farid, A.M. Khudhair, S.A.K. Razack, S. Al-Hallaj, Review on phase change energy storage: materials and applications, Energy Convers. Manage. 45 (2004) 1597–1615.
[14] K. Faraj, M. Khaled, J. Faraj, F. Hachem, C. Castelaine, A review on phase change materials for thermal energy storage in buildings: heating and hybrid applications, J. Energy Storage 33 (2021) 101913.
[15] A. de Gracia, L. Navarro, A. Castell, A. Ruiz-Pardo, S. Álvarez, L.F. Cabeza, Thermal analysis of a ventilated facade with PCM for cooling applications, Energy Build. 65 (2013) 508–515.
[16] A. de Gracia, L. Navarro, A. Castell, A. Ruiz-Pardo, S. Álvarez, L.F. Cabeza, Experimental study of a ventilated facade with PCM during winter period, Energy Build. 58 (2012) 324–332.
[17] G. Diarce, A. Urresti, A. García-Romero, A. Delgado, A. Erkoreka, C. Escudero, Á. Campos-Celador, Ventilated active façades with PCM, Appl. Energy 109 (2013) 530–537.
[18] D. Feldman, D. Banu, D. Hawes, E. Ghanbari, Obtaining an energy storing building material by direct incorporation of an organic phase change material in gypsum wallboard, Sol. Energy Mater. 22 (1991) 231–242.
[19] R. Barzin, J.J.J. Chen, B.R. Young, M.M. Farid, Application of PCM energy storage in combination with night ventilation for space cooling, Appl. Energy 158 (2015) 412–421.
[20] X. Wang, H. Yu, L. Li, M. Zhao, Experimental assessment on the use of phase change materials, (PCMs)-bricks in the exterior wall of a full-scale room, Energy Convers. Manag. 120 (2016) 81–89.
[21] S.A. Memon, H.Z. Cui, H. Zhang, F. Xing, Utilization of macro encapsulated phase change materials for the development of thermal energy storage and structural lightweight aggregate concrete, Appl. Energy 139 (2015) 43–55.
[22] Y.P. Zhang, K.P. Lin, R. Yang, H.F. Di, Y. Jiang, Preparation, thermal performance and application of shape-stabilized PCM in energy efficient buildings, Energy Build. 38 (2006) 1262–1269.
[23] U. Berardi, A.A. Gallardo, Properties of concretes enhanced with phase change materials for building applications, Energy Build. 199 (2019) 402–414.
[24] E.M. Alawadhi, Thermal analysis of a building brick containing phase change material, Energy Build. 40 (2008) 351–357.
[25] R. Vicente, T. Silva, Brick masonry walls with PCM macrocapsules: an experimental approach, Appl. Therm. Eng. 67 (2014) 24–34.
[26] B. Maleki, A. Khadang, H. Maddah, M. Alizadeh, A. Kazemian, H.M. Ali, Development and thermal performance of nanoencapsulated PCM/ plaster wallboard for thermal energy storage in buildings, J. Build. Eng. 32 (2020)101727.
[27] I. Cerón, J. Neila, M. Khayayet, Experimental tile with phase change materials (PCM) for building use, Energy Build. 43 (2011) 1869–1874.
[28] M. Ryms, W.M. Lewandowski, E. Klugmann-Radziemska, H. Denda, P. Wcisło, The use of lightweight aggregate saturated with PCM as a temperature stabilizing material for road surfaces, Appl. Therm. Eng. 81 (2015) 313–324.

[29] R.M. Novais, G. Ascensão, M.P. Seabra, J.A. LabrinchaMaterials, Lightweight dense/porous PCM-ceramic tiles for indoor temperature control, Energy Build. 108 (2015) 205–214.
[30] R.M. Novais, M.P. Seabra, J.A. Labrincha, Lightweight dense/porous bi-layered ceramic tiles prepared by double pressing, J. Mater. Process. Technol. 216 (2015) 169–177.
[31] C. Bories, M.E. Borredon, E. Vedrenne, G. Vilarem, Development of eco-friendly porous fired clay bricks using pore-forming agents: a review, J. Environ. Manag. 143 (2014) 186–196.
[32] M. Marangoni, M. Secco, M. Parisatto, G. Artioli, E. Bernardo, P. Colombo, H. Altlasi, M. Binmajed, M. Binhussain, Cellular glass–ceramics from a self foaming mixture of glass and basalt scoria, J. Non-Cryst. Solids 403 (2014) 38–46.
[33] R.R. Petersen, J. König, Y. Yue, The viscosity window of the silicate glass foam production, J. Non-Cryst. Solids 456 (2017) 49–54.
[34] C. Molinari, C. Zanelli, G. Guarini, M. Dondi, Bloating mechanism in lightweight aggregates: effect of processing variables and properties of the vitreous phase, J. Build. Constr. Plan. Mater. Res. 261 (2020) 9 119980.
[35] C. Piselli, M. Prabhakar, A. de Gracia, M. Saffari, A.L. Pisello, L.F. Cabeza, Optimal control of natural ventilation as passive cooling strategy for improving the energy performance of building envelope with PCM integration, Renew. Energy 162 (2020) 171–181.
[36] J. Čurpek, M. Čekon, Climate response of a BiPV façade system enhanced with latent PCM-based thermal energy storage, Renew. Energy 152 (2020) 368–384.
[37] M. Ahangari, M. Maerefat, An innovative PCM system for thermal comfort improvement and energy demand reduction in building under different climate conditions, Sustain. Cities Soc. 44 (2019) 120–129.
[38] D. Li, Y. Wu, G. Zhang, M. Arıcı, C. Liu, F. Wang, Influence of glazed roof containing phase change material on indoor thermal environment and energy consumption, Appl. Energy 222 (2018) 343–350.
[39] L. Laghi, F. Pennecchi, G. Raiteri, Uncertainty analysis of thermal conductivity measurements in materials for energy-efficient buildings, Int. J. Metrol. Qual. Eng. 2 (2011) 141–151.
[40] H. Wang, Z. Chen, L. Liu, R. Ji, X. Wang, Synthesis of a foam ceramic based on ceramic tile polishing waste using SiC as foaming agent, Ceram. Int. 44 (2018) 10078–10086.
[41] J. König, R.R. Petersen, Y. Yue, Influence of glass-calcium carbonate mixture's characteristics on the foaming process and the properties of the foam glass, J. Eur. Ceram. Soc. 34 (2014) 1591–1598.
[42] Y. Yang, Weidong Wu, S. Fu, H. Zhang, Study of a novel ceramsite-based shape-stabilized composite phase change material (PCM) for energy conservation in buildings, Constr. Build. Mater. 246 (2020)118479.b:maintitle>246(2020) 118479.